

Electronic Supplementary Information

Bimetallic Pd₉₆Fe₄ Nanodendrites Embedded in Graphitic Carbon Nanosheets as Highly Efficient Anode Electrocatalysts

Srabanti Ghosh^{a,*}, Sandip Bysakh^b, Rajendra Nath Basu^{a*}

^aFuel Cell and Battery Division, CSIR - Central Glass and Ceramic Research Institute,

^bMaterials Characterization Division, CSIR - Central Glass and Ceramic Research Institute
196, Raja S. C. Mullick Road, Kolkata-700032, India

*Corresponding Authors Email: ghosh.srabanti@gmail.com

rnbasu@cgcri.res.in

List of contents:

Fig.S1 (a) FESEM image of mesocarbon microbeads (MCMB). (b) TEM and (c) HRTEM image of graphitic carbon nanosheets derived after radiolysis of MCMB solution.

Fig.S2 (a) TEM, (b) HRTEM, (c) HAADF-STEM images, and (d, e) elemental mapping and (f) EDS line scanning profiles of Pd₇₇Fe₂₃/GCN nanohybrids.

Fig.S3 A typical Raman spectrum of Pd₉₆Fe₄/GNC nano hybrid.

Fig.S4 Cyclic voltammetric runs associated with the electrocatalytic oxidation of 0.5 M EtOH by Fe₁₀₀/GCN in 1 M KOH. The reference electrode was Hg/HgO electrode. The scan rate was 50 mVs⁻¹.

Fig.S5 (a) Long cycling study of Pd₉₆Fe₄/GCN electrodes in a solution of 1M KOH and 0.5 M ethanol at scan rate of 50 mV Sec⁻¹.

Fig.S6 (a) Long cycling study of Pd/C, Pd/GCN, and Pd₉₆Fe₄/GCN electrodes in a solution of 1M KOH and 0.5 M ethanol at scan rate of 50 mV Sec⁻¹. (b) XRD, (c) FESEM (d) TEM images of Pd₉₆Fe₄/GCN electrodes after 1000 cycling of ethanol oxidation.

Fig.S7 Cyclic voltammograms for Pd₉₆Fe₄/GCN catalyst for CH₃CH₂OH, CH₃CHO, and CH₃COONa solutions fuels each of concentration 100 mM in 0.5 M aqueous KOH at a scan rate of 50 mV Sec⁻¹.

Table S1 Elemental compositions of Pd-Fe contained nanoalloys measured by ICP-AES.

Table S2 Comparison of the electrochemical performance of Pd electrocatalysts for the ethanol oxidation.

Table S3 Effect of catalysts for the oxidation of methanol, ethylene glycol, tri-ethylene glycol, glycerol.

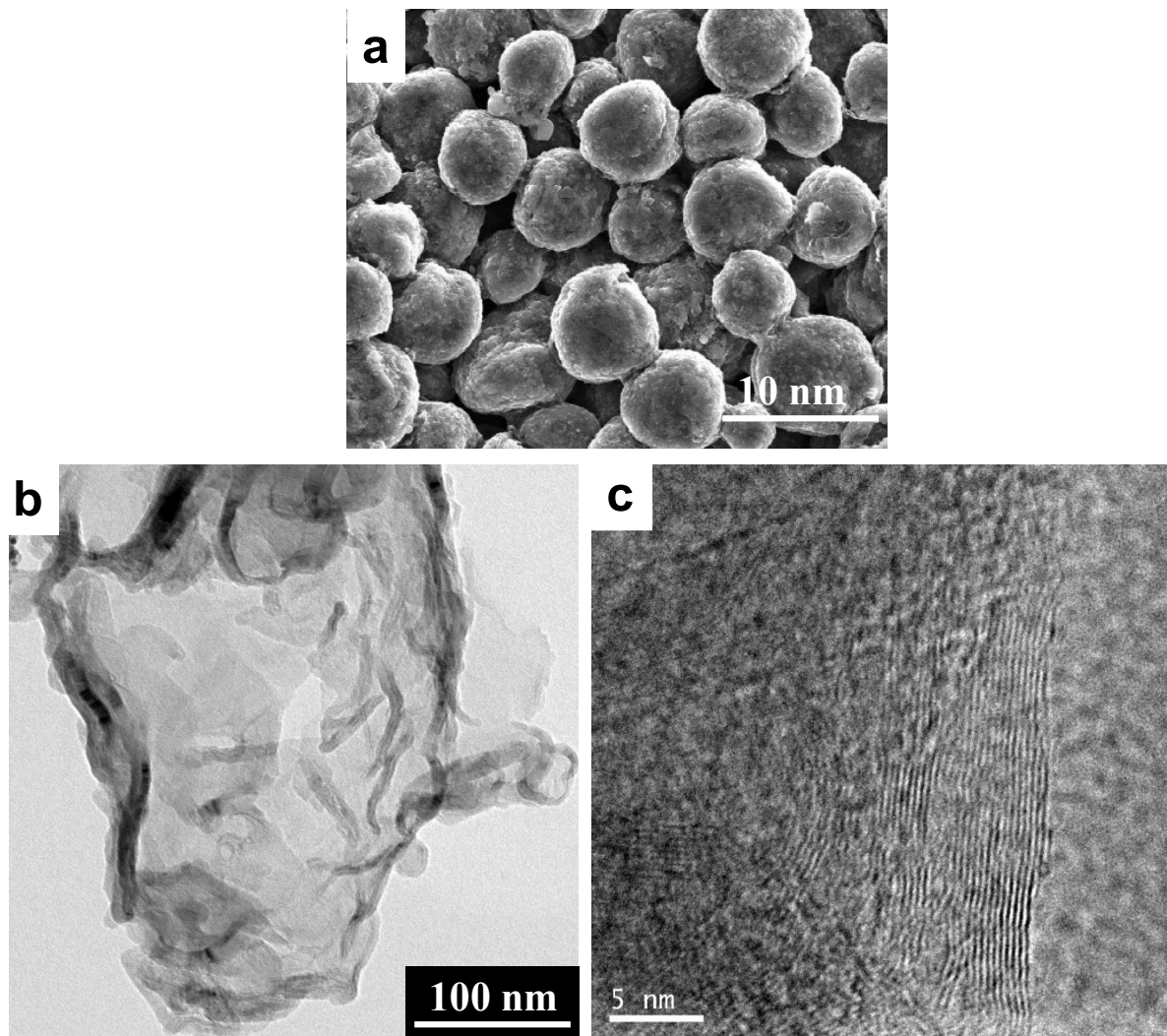


Fig.S1 (a) FESEM image of mesocarbon microbeads (MCMB). (b) TEM and (c) HRTEM image of graphitic carbon nanosheets derived after radiolysis of MCMB solution.

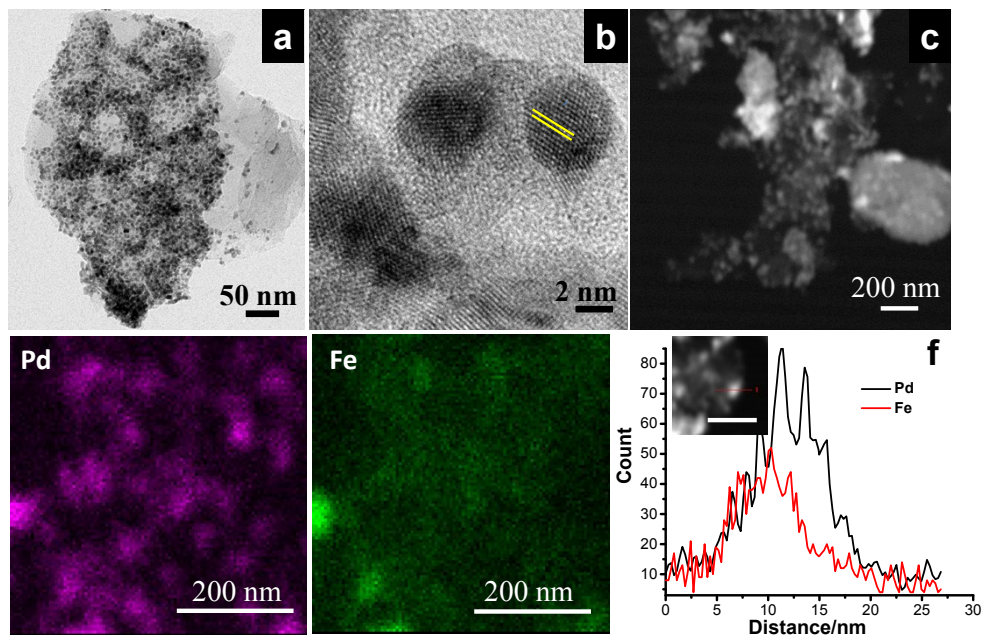


Fig.S2 (a) TEM, (b) HRTEM, (c) HAADF-STEM images, and (d, e) elemental mapping and (f) EDS line scanning profiles of $\text{Pd}_{77}\text{Fe}_{23}/\text{GCN}$ nanohybrids.

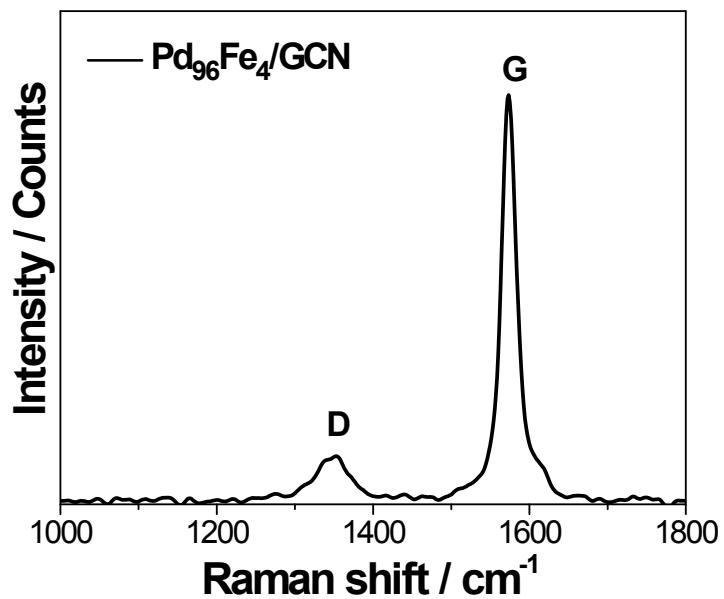


Fig.S3 A typical Raman spectrum of $\text{Pd}_{96}\text{Fe}_{4}/\text{GNC}$ nanohybrid.

Table S1 Elemental compositions of Pd-Fe contained nanoalloys measured by ICP-AES.

Metal loaded on GCN	ICP-AES		Metal composition in solution		Metal content by ICP-AES
	Atomic content (at.%)		(Atomic, at.%)		Weight (%)
	Pd	Fe	Pd	Fe	
Pd	100	-	-	100	9±1%
Fe	-	100	100	-	1.5±0.35%
Pd ₉₆ Fe ₄	96±2.1	4±1.5	90	10	4±0.15%
Pd ₉₁ Fe ₉	91±3.2	9±1.8	85	15	3.4±.28%
Pd ₈₅ Fe ₁₅	85±3.7	15±2.8	75	25	1.9±0.5%
Pd ₇₇ Fe ₂₃	77±4.8	23±2.1	50	50	1.45±0.12%

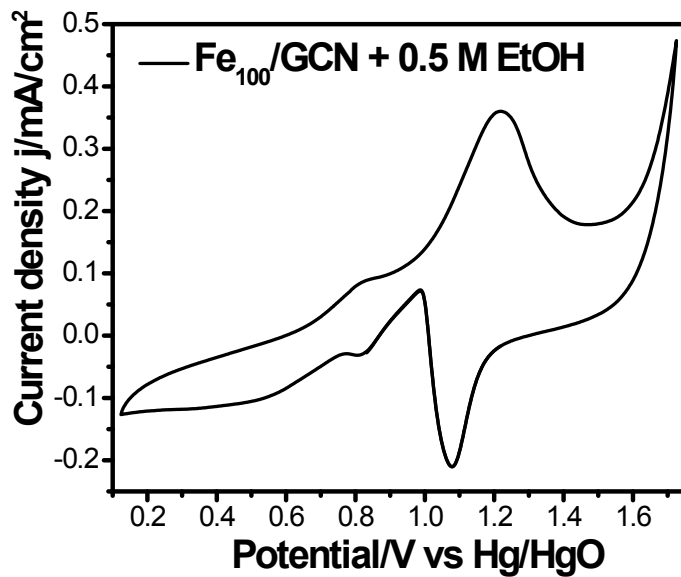


Fig.S4 Cyclic voltammetric runs associated with the electrocatalytic oxidation of 0.5 M EtOH by Fe₁₀₀/GCN in 1 M KOH. The reference electrode was Hg/HgO electrode. The scan rate was 50 mVs⁻¹.

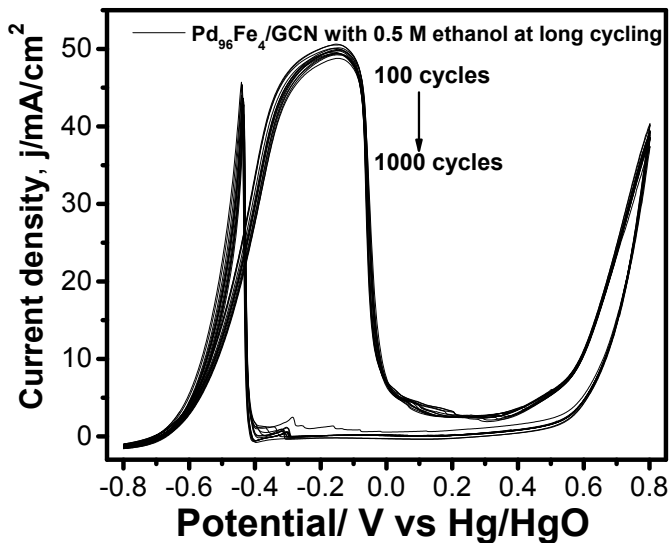


Fig.S5 (a) Long cycling study of $\text{Pd}_{96}\text{Fe}_4/\text{GCN}$ electrodes in a solution of 1M KOH and 0.5 M ethanol at scan rate of 50 mV Sec⁻¹.

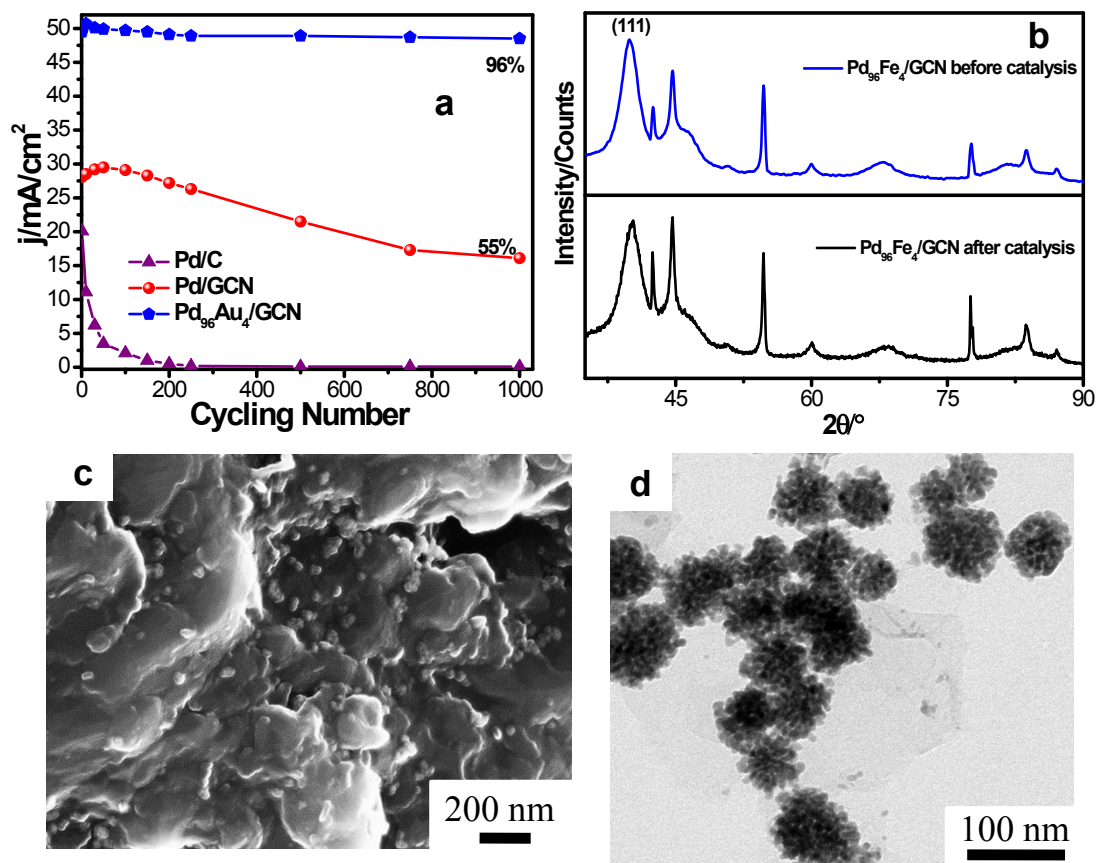


Fig.S6 (a) Long cycling study of Pd/C, Pd/GCN, and $\text{Pd}_{96}\text{Fe}_4/\text{GCN}$ electrodes in a solution of 1M KOH and 0.5 M ethanol at scan rate of 50 mV Sec⁻¹. (b) XRD, (c) FESEM (d) TEM images of $\text{Pd}_{96}\text{Fe}_4/\text{GCN}$ electrodes after 1000 cycling of ethanol oxidation.

Table S2 Comparison of the electrochemical performance of Pd electrocatalysts for the ethanol oxidation.

Electrode	E_{onset} , mV/RHE	j_f , mA.cm ⁻²	j_f , mA.cm ⁻² .mg ⁻¹	Specific Current, j_f , mA.mg ⁻¹	Reference
Pd black catalyst	-306	0.65	-	-	1
Pd/Graphene	-356	0.56	-	-	2
Pd/CNT	-320	-	364	-	3
Pd/C	-436	-	63	-	4
Pd/C	-335	-	42	-	5
Pd/Ppy	-384	7.05	4147	248.70	6
Pd/Graphene/Nafion	-376	14.22	5925	355.5	7
Pd/Nafion	-346	8.55	1745	104.7	7
Pd nanoplates/Nafion	-376	4.05	1500	90	8
Pd nanowires/Nafion	-420	-	1327	-	9
Pd/CNT	-426	-	3540	-	10
PtPdNPs/GNs	-	22.4	-	-	11
Ni@PbPt/Graphene	-	-	-	281	12
Pt–Pd (1:3)/RGO	-	-	-	1486.7	13
Pt–Cu/RGO	-	-	-	1114.7	14
PtPd NFs-RGO	-	-	-	600	15
PdCo NTAs/CFC	-	-	-	1491	16
Pd/PANI/Pd	-	-	-	310	17
Pd–PEDOT/GE	-	-	-	458.5	18
Pd–PEDOT	-	-	-	285.1	18
PtPd/PPy/PtPd nanotube	-	3.1	-	-	19
Pd ₈₉ Pt ₁₁ /PPy	-356	15.8	5197	782	20
Pd ₅₄ Au ₄₆ /PPy	-426	10.35	5280	792	20
Pd ₉₆ Fe ₄ /GCN	-486	49.8	11008	1100	This work

Table S3 Effect of catalysts for the oxidation of methanol, ethylene glycol, tri-ethylene glycol, glycerol.

Fuel	Current density (mA/cm^2)				
	Pd ₁₀₀ /GCN	Pd ₉₆ Fe ₄ /GCN	Pd ₉₁ Fe ₉ /GCN	Pd ₈₅ Fe ₁₅ /GCN	Pd ₇₇ Fe ₂₃ /GCN
Ethanol	30.2	49.87	32.4	24.1	18.5
Methanol	1.87	5.38	4.7	4.4	4.023
Ethylene Glycol	12.8	22.63	7.9	7.8	3.48
Tri-Ethylene Glycol	0.88	1.29	0.84	0.33	0.13
Glycerol	2.75	8.37	7.08	7.70	4.3

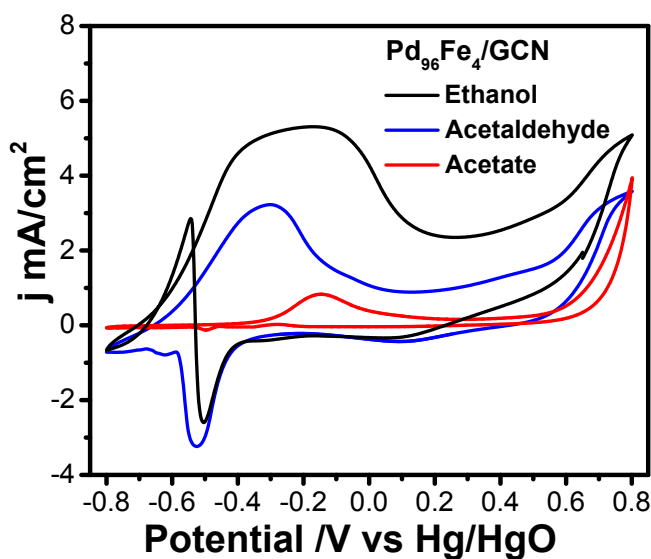


Fig.S7 Cyclic voltammograms for Pd₉₆Fe₄/GCN catalyst for CH₃CH₂OH, CH₃CHO, and CH₃COONa solutions fuels each of concentration 100 mM in 0.5 M aqueous KOH at a scan rate of 50 mV Sec⁻¹.

References

1. N. Tian, Z.-Y. Zhou, N.-F. Yu, L.-Y. Wang, S.-G. Sun, *J. Am. Chem. Soc.*, 2010, **132**, 7580–7581.
2. Q. Zhang, E. Uchaker, S. L. Candelaria and G. Cao, *Chem. Soc. Rev.*, 2013, **42**, 3127–3171.
3. N. Mackiewicz, G. Surendran, H. Remita, B. Keita, G. Zhang, L. Nadjo, A. Hagège, E. Doris and C. Mioskowski, *J. Am. Chem. Soc.*, 2008, **130**, 8110–8111.
4. C. Xu and P. K. Shen, Liu, Y. *J. Power Sources*, 2007, **164**, 527–531.
5. M. Grde'n, M. Łukaszewski, G. Jerkiewicz and A. Czerwiński, *Electrochim. Acta*, 2008, **53**, 7583–7598.
6. S. Ghosh, N. Bhandary, S. Basu and R. N. Basu, *Electrocatalysis*, 2017, **8**, 329–339.
7. S. Ghosh, H. Remita, P. Kar, S. Choudhury, S. Sardar, P. Beaunier, P. S. Roy, S. K. Bhattacharya and S. K. Pal, *J. Mater. Chem. A*, 2015, **3**, 9517–9527.
8. S. Ghosh, A.-L. Teillout, D. Floresyona, Pedro de Oliveira, A. Hagège and H. Remita, *Int. J. Hydrogen Energy*, 2015, **40**, 4951–4959.
9. F. Ksar, G. Surendran, L. Ramos, B. Keita, L. Nadjo, E. Prouzet, P. Beaunier, A. Hagège, F.; Audonnet and H. Remita, *Chem. Mater.* 2009, **21**, 1612–1617.
10. N. Mackiewicz, G. Surendran, H. Remita, B. Keita, G. Zhang, L. Nadjo, A. Hag'ege, E. Doris and C. Mioskowski, *J. Am. Chem. Soc.*, 2008, **130**, 8110–8111.
11. X. Chen, Z. Cai, X. Chen and M. Oyama, *J. Mater. Chem. A*, 2014, **2**, 315–320.
12. D. Chen, Y. Zhao, Y. Fan, X. Peng, X. Wang and J. Tian, *J. Mater. Chem. A*, 2013, **1**, 13227–13232.
13. J.-J. Lv, N. Wisitruangsakul, J.-J. Feng, J. Luo, K.-M. Fang and A.-J. Wang, *Electrochim. Acta*, 2015, **160**, 100–107.
14. J.-J. Lv, J.-N. Zheng, L.-L. Chen, M. Lin, A.-J. Wang, J.-R. Chen and J.-J. Feng, *Electrochim. Acta*, 2014, **143**, 36–43.
15. M. Gong, Z. Yao, F. Lai, Y. Chen and Y. Tang, *Carbon*, 2015, **91**, 338–345.

16. A. L. Wang, X. J. He, X. F. Lu, H. Xu, Y. X. Tong and G. R. Li, *Angew. Chem. Int. Ed.*, 2015, **54**, 3669–3673.
17. A.-L. Wang, H. Xu, J.-X. Feng, L.-X. Ding, Y.-X. Tong and G.-R. Li, *J. Am. Chem. Soc.*, 2013, **135**, 10703–10709.
18. H. Xu, L.-X. Ding, C.-L. Liang, Y.-X. Tong and G.-R. Li, *NPG Asia Mater.*, 2013, **5**, e69–e72.
19. R. Yue, H. Wang, D. Bin, J. Xu, Y. Du, W. Lu and J. Guo, *J. Mater. Chem. A*, 2015, **3**, 1077–1088.
20. S. Ghosh, S. Bera, S. Bysakh and R. N. Basu, *ACS Appl. Mater. Interfaces*, 2017, **9**, 33775–33790.